

### Electronic Supplementary Information

#### **An enzyme-free DNA circuit for the amplified detection of Cd<sup>2+</sup> based on hairpin probe-mediated toehold binding and branch migration**

Jiafeng Pan,<sup>a,b,#</sup> Lingwen Zeng,<sup>a,#</sup> and Junhua Chen<sup>\*b</sup>

<sup>a</sup>School of Food Science and Engineering, Foshan University, Foshan 528000, China.

<sup>b</sup>Guangdong Key Laboratory of Integrated Agro-environmental Pollution Control and Management, Guangdong Institute of Eco-environmental Science & Technology, Guangzhou 510650, China.

#The two authors contributed equally to this work.

\*Corresponding author

E-mail: 222chenjunhua@163.com

## Experimental Section

### Reagents and materials

*N*-methyl mesoporphyrinIX (NMM), ammonium persulfate (APS), SYBR Green, Tris, and *N,N,N',N'*-tetramethylethylenediamine (TEMED) were purchased from Sigma-Aldrich (St. Louis, Mo). A NMM stock solution (5 mM) was prepared in DMSO and stored in the dark at -20 °C. Other chemicals were of analytical grade without further purification. Ultrapure water (18.2 MΩ/cm) was used to prepare the buffer solution. The HPLC-purified oligonucleotides were produced by Sangon Biotech. Co. Ltd. (Shanghai, China) and the oligonucleotide sequences were listed as follows:



## **Apparatus**

The fluorescence measurements were carried out on the SpectraMax i3x (Molecular Devices, the U. S.) during the experiments. The polyacrylamide gel electrophoresis (PAGE) experiments were run by the PowerPac electrophoresis apparatus (BIO-RAD, Singapore).

## **Analytical procedure**

All of the oligonucleotides were dissolved into 50 mM Tris-HCl buffer (pH 7.6, containing 5 mM MgCl<sub>2</sub>, 150 mM NaCl, and 50 mM KCl). Subsequently, H1 and H2 were heated to 97 °C for 5 min and then slowly cooled down to room temperature for the forming hairpin probes. 200 nM aptamer, 500 nM H1, and 1000 nM H2 were mixed with different concentrations of Cd<sup>2+</sup> and incubated for 120 min at room temperature. Then, 1.5 μM NMM were added into the resulting solution before measurements. The fluorescence spectra were recorded with the excitation wavelength of 399 nm.

To investigate the specificity of the assay, other metal ions including As<sup>3+</sup>, Ag<sup>+</sup>, Mg<sup>2+</sup>, Fe<sup>2+</sup>, Mn<sup>2+</sup>, Ni<sup>2+</sup>, Ca<sup>2+</sup>, Cu<sup>2+</sup>, Zn<sup>2+</sup>, and Hg<sup>2+</sup> were tested in the same way.

## **Analysis of real samples**

The river water was collected from Pearl River (Guangzhou, China). The tap water was collected from our lab. The lake water was collected from South China Botanical Garden (Guangzhou, China). The pond water was collected from our institute. Human serums were provided by the 4th Affiliated Hospital of Guangzhou Medical University (Guangzhou, China). The samples were filtered with 0.22 μm microfiltration membrane to remove the solid impurities and suspension. The concentration of Cd<sup>2+</sup> in the real samples was detected using our proposed biosensor. Also, AFS assay was employed to verify the biosensor results.

## **Polyacrylamide gel electrophoresis (PAGE) analysis**

The 8 % PAGE gel was prepared for electrophoresis analysis. 6.13 mL of ultrapure water, 100 μL of APS (10%), 1 mL of 10 × TBE buffer, 2.67 mL of 30% Acr-bis (29:1), and 4 μL of TEMED were mixed and polymerized at 25 °C for 1 h. Then, the loading sample was prepared by mixing 5 μL the resulting solution and 1 μL 6 × loading buffer. Subsequently, the electrophoresis experiments

were carried out at 45 V for 90 min in  $1 \times$  TBE buffer. Finally, the PAGE gel was stained in diluted SYBR Green solution, and then photographed in a gel image system (Bio-Rad, Singapore).

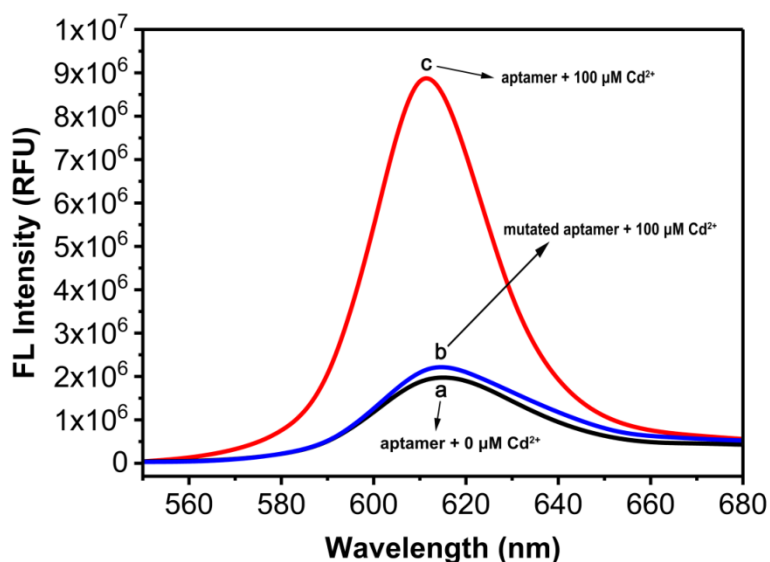


Fig. S1. The fluorescence signal of the sensing system using the  $\text{Cd}^{2+}$ -specific aptamer or the mutated aptamer sequence as the binding element: (a) no  $\text{Cd}^{2+}$  + 200 nM  $\text{Cd}^{2+}$ -specific aptamer + 500 nM H1 + 1000 nM H2, (b) 100  $\mu\text{M}$   $\text{Cd}^{2+}$  + 200 nM mutated aptamer sequence + 500 nM H1 + 1000 nM H2, and (c) 100  $\mu\text{M}$   $\text{Cd}^{2+}$  + 200 nM  $\text{Cd}^{2+}$ -specific aptamer + 500 nM H1 + 1000 nM H2.

To verify the specific binding between the aptamer and  $\text{Cd}^{2+}$ , another mutated aptamer sequence was used to replace the correct aptamer in the sensing system. As shown in Fig. S1 (ESI<sup>+</sup>), the correct aptamer can bind with  $\text{Cd}^{2+}$  and generate a high fluorescence response signal (curve c). while the mutated aptamer sequence failed to bind with  $\text{Cd}^{2+}$ , and only very weak signal can be observed (curve b), which is almost as the same as the blank sample (curve a).

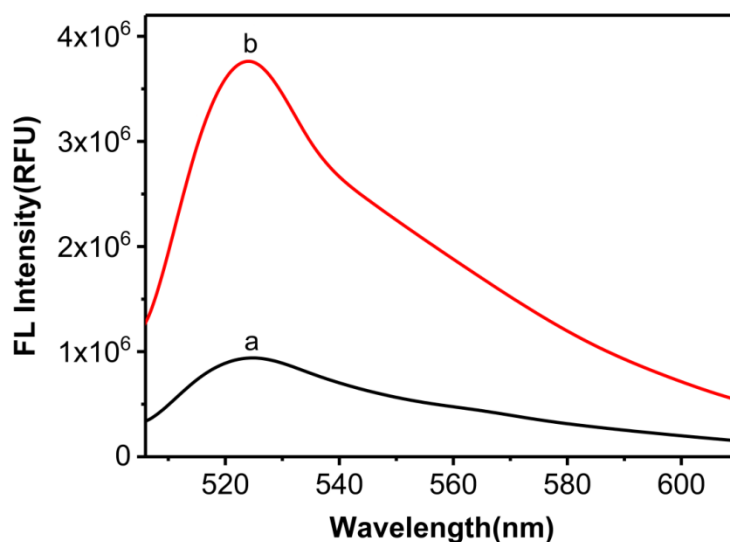


Fig. S2. The fluorescence response of the aptamer solution (a) and the aptamer + Cd<sup>2+</sup> solution (b) using SYBR Green I as the fluorescence dye. The aptamer concentration, 200 nM. Cd<sup>2+</sup> concentration, 100 nM.

SYBR Green I, a double-stranded DNA (dsDNA) specific dye, was applied for the readout fluorescence signal to confirm the conformation change of the aptamer after binding with Cd<sup>2+</sup>. As show in Fig. S2 (ESI<sup>+</sup>), the aptamer without Cd<sup>2+</sup> only displayed a weak fluorescence background signal (curve a). This indicated that in the absence of Cd<sup>2+</sup>, the aptamer was kept almost as a single-stranded DNA (ssDNA) state. As SYBR Green I stains ssDNA with much lower intensity than dsDNA, only weak fluorescence background signal can be detected. When Cd<sup>2+</sup> was added into the aptamer solution, a hairpin structure containing part ssDNA would be generated, thereby greatly enhancing the fluorescence intensity of DNA intercalator SYBR Green I (curve b).

To obtain the optimal assay conditions for  $\text{Cd}^{2+}$  detection, some experimental parameters including the concentration of H2, the reaction temperature, the incubation time, and the concentration of NMM were optimized. As shown in Fig. S3 (ESI<sup>+</sup>), the optimal concentration of H2 was 1000 nM. As shown in Fig. S4 (ESI<sup>+</sup>), 25°C was chosen as the optimal reaction temperature. As shown in Fig. S5 (ESI<sup>+</sup>), 120 min was employed as the optimal incubation time on the signal amplification process. As shown in Fig. S6 (ESI<sup>+</sup>), the optimal concentration of NMM was 1.5  $\mu\text{M}$ .

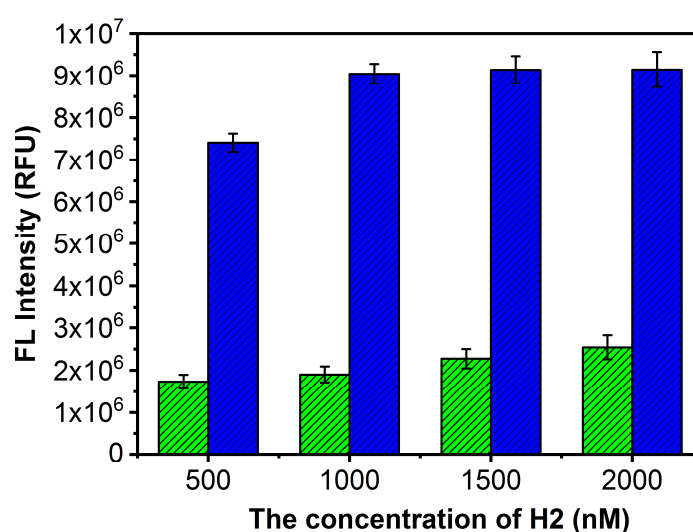


Fig. S3. Effect of the concentration of H2 on the performance of the sensing system. The histograms represent the fluorescence intensities of the solution with 100  $\mu\text{M Cd}^{2+}$  (blue) and without  $\text{Cd}^{2+}$  (green), respectively. The experiments were performed at room temperature (25°C). Error bars represent the standard deviation of three independent measurements.

The effect of the concentration of H2 was evaluated by detecting 100  $\mu\text{M Cd}^{2+}$ . As shown in Fig. S3 (ESI<sup>+</sup>), the fluorescence intensity remained almost unchanged when the concentration of H2 is higher than 1000 nM. However, the background was continuously elevated with increasing H2 concentration. Therefore, 1000 nM of H2 was set as the optimal concentration in our study.

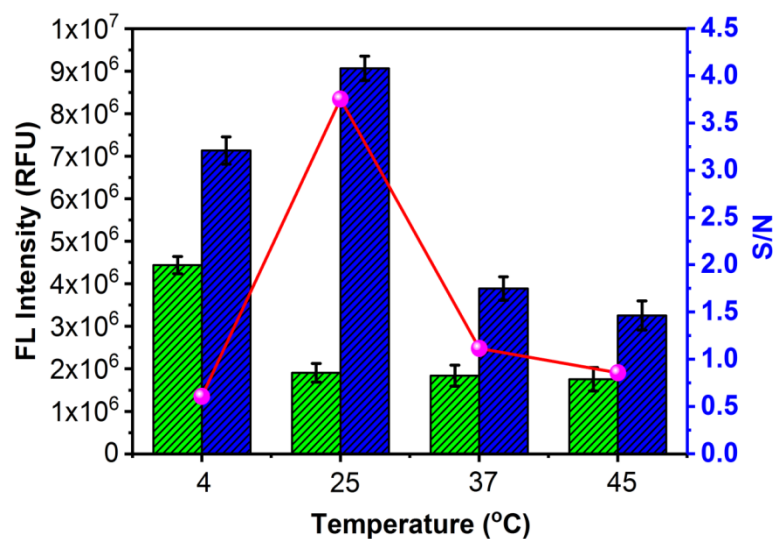


Fig. S4. Effect of the temperature on the performance of the sensing system. The histograms represent the fluorescence intensities of the solution with 100  $\mu\text{M}$   $\text{Cd}^{2+}$  (blue) and without  $\text{Cd}^{2+}$  (green), respectively. The red line represents the S/N ratio. The solution contains 200 nM aptamer, 500 nM H1, and 1000 nM H2. Error bars represent the standard deviation of three independent measurements.

The effect of the reaction temperature on the response of the biosensor was also investigated by detecting 100  $\mu\text{M}$   $\text{Cd}^{2+}$  at different temperatures (4°C, 25°C, 37°C, and 45°C). As shown in Fig. S4 (ESI<sup>†</sup>), the maximum signal-to-noise (S/N) ratio was obtained at 25°C. The formed H1-H2 product will become unstable when the temperature was higher than 25°C. On the other hand, the background signal increased at 4°C because the H1-H2 may be formed through the hybridization between H1 and H2 even in the absence of  $\text{Cd}^{2+}$ . Thus, 25°C was chosen as the optimal reaction temperature.

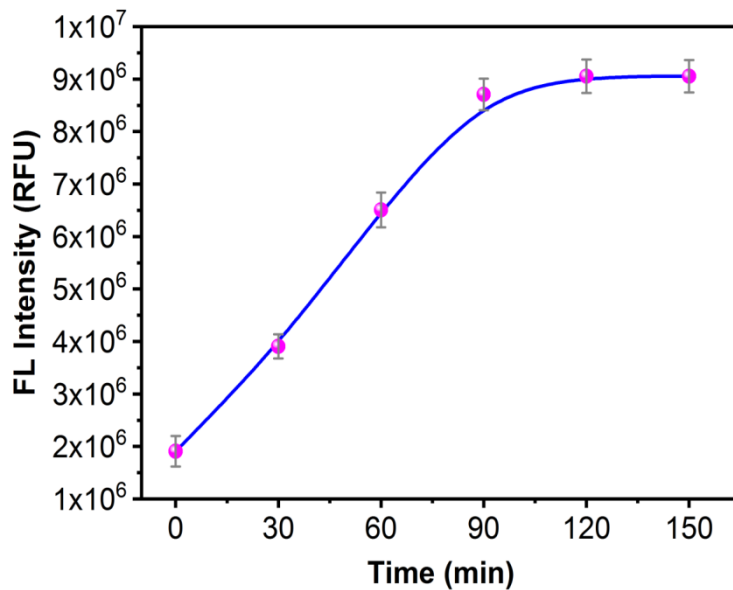


Fig. S5. Effect of the incubation time on the performance of the sensing system. The solution contains 100  $\mu\text{M}$   $\text{Cd}^{2+}$ , 200 nM aptamer, 500 nM H1, and 1000 nM H2. The experiments were performed at room temperature (25°C). Error bars represent the standard deviation of three independent measurements.

Furthermore, the effect of incubation time on the signal amplification process was also explored. According to the results in Fig. S5 (ESI<sup>+</sup>), the fluorescence intensity initially increased with increasing the incubation time and then achieved a plateau after 120 min, indicating that our assay can be finished within 120 min. To ensure the signal amplification reactions can be carried out completely, 120 min was employed as the optimal incubation time.



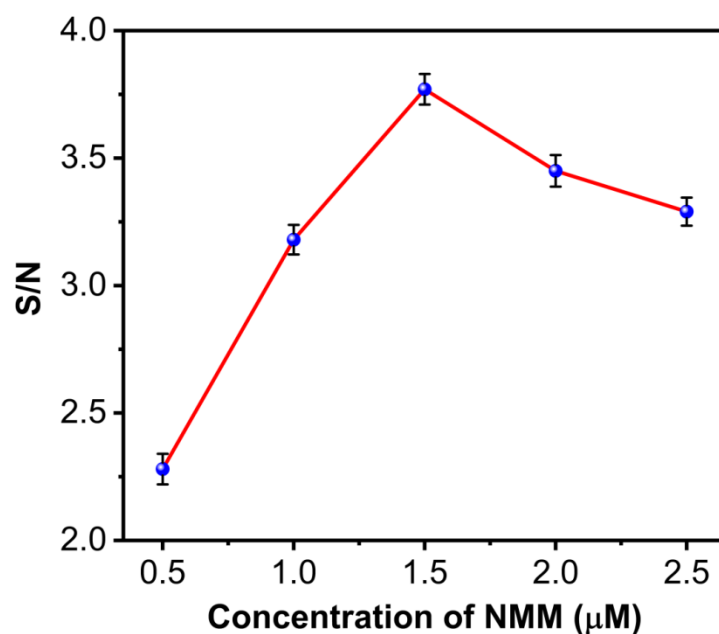


Fig. S6. The effect of the concentration of NMM on the biosensor response. The solution contains 200 nM aptamer, 500 nM H1, 1000 nM H2, and 100  $\mu\text{M}$   $\text{Cd}^{2+}$  or without  $\text{Cd}^{2+}$ . Error bars represent the standard deviation of three independent measurements.

The effect of the NMM concentration on the biosensor response was optimized. As shown in Fig. S6 (ESI<sup>+</sup>), the S/N ratio increased with increasing the concentration of NMM from 0.5 to 1.5  $\mu\text{M}$ . Further increasing the NMM concentration will result in the decrease of the S/N ratio. Thus, the optimal concentration of NMM was 1.5  $\mu\text{M}$ .

Table S1. Comparison of some currently available methods for the detection of Cd<sup>2+</sup>.

Method	Strategy	LOD	Ref.
Fluorescent	Tetraphenylethene-Triazole-cyclodextrin	10 nM	[1]
Fluorescent	Phosphorothioate modified DNAzyme	4.8 nM	[2]
Luminescent	S <sup>2-</sup> capped CdSe/CdSeS/CdS NCs	110 pM	[3]
Electrochemical	Aptamer labeled AuNPs	0.62 pM	[4]
Electrochemical	Paper-based ion-selective electrodes	1.2 nM	[5]
Photoelectrochemical	Zn doped CdS	0.35 nM	[6]
Colorimetric	EDTA-BSA functionalized AuNPs	0.89 nM	[7]
Colorimetric	Au@g-CNQDs	10 nM	[8]
SERS	Trithiocyanuric modified AuNPs	2.9 nM	[9]
Fluorescent	Aptamer and DNAzyme	50 pM	[This work]

Table S2. Application of the proposed biosensor for Cd<sup>2+</sup> determination in human urine and river water.

Sample	Added (nM)	Found <sup>a</sup> (nM)	Recovery <sup>a</sup> (%)	Found <sup>b</sup> (nM)	Recovery <sup>b</sup> (%)
1	20.0	20.9	104.5	19.6	95.3
2	40.0	42.4	106.0	41.3	103.3
3	60.0	64.1	106.8	63.1	105.2
4	80.0	77.8	97.25	85.6	107.0
5	100.0	96.9	96.9	99.7	99.7

<sup>a</sup>Each sample was analyzed in human urine, and all values were obtained as an average of three repetitive determinations. <sup>b</sup>Each sample was analyzed in river water, and all values were obtained as an average of three repetitive determinations.

Table S3. Determination of Cd<sup>2+</sup> in water samples using the proposed biosensor and AFS method.

Sample	Proposed method <sup>a</sup> (nM)	AFS <sup>b</sup> (nM)	Relative error (Re) <sup>c</sup> (%)
Tap water	0.73	0.69	-5.8
Lake water	3.62	3.77	4.0
Pond water	9.84	10.39	5.3

<sup>a</sup>Each sample was analyzed using our proposed fluorescence biosensor, and all values were obtained as an average of three repetitive determinations. <sup>b</sup>Each sample was analyzed using the AFS (atomic fluorescence spectrometer), and all values were obtained as an average of three repetitive determinations. <sup>c</sup>Our proposed method vs. AFS.

## References

- 1 L. Zhang, W. Hu, L. Yu and Y. Wang, *Chem. Commun.*, 2015, **51**, 4298-4301.
- 2 P. J. Huang and J. Liu, *Anal. Chem.*, 2014, **86**, 5999-6005.
- 3 A. Swarnkar, G. S. Shanker and A. Nag, *Chem. Commun.*, 2014, **50**, 4743-4746.
- 4 W. Tang, Z. Wang, J. Yu, F. Zhang and P. He, *Anal. Chem.*, 2018, **90**, 8337-9344.
- 5 Q. Sun, J. Wang, M. Tang, L. Huang, Z. Zhang, C. Liu, X. Lu, K. W. Hunter and G. Chen, *Anal. Chem.*, 2017, **89**, 5024-5029.
- 6 Y. Zhang, H. Ma, D. Wu, R. Li, X. Wang, Y. Wang, W. Zhu, Q. Wei and B. Du, *Biosens. Bioelectron.*, 2016, **77**, 936-941.
- 7 A. M. L. Marzo, J. Pons, D. A. Blake and A. Merkoci, *Biosens. Bioelectron.*, 2013, **47**, 190-198.
- 8 Z. Zhang, Z. Zhang, H. Liu, X. Mao, W. Liu, S. Zhang, Z. Nie and L. Lu, *Biosens. Bioelectron.*, 2018, **103**, 87-93.
- 9 Y. Chen, Z. Chen, S. Long and R. Yu, *Anal. Chem.*, 2014, **86**, 12236-12242.